Environmental Pollution 265 (2020) 114996

Contents lists available at ScienceDirect

Environmental Pollution

journal homepage: www.elsevier.com/locate/envpol

Pilot-scale study on the effects of cyanobacterial blooms on *Vallisneria natans* and biofilms at different phosphorus concentrations

Qi Li , Peng Gu , Xin Luo , Hao Zhang , Suzhen Huang , Jibiao Zhang , Zheng Zheng *

Department of Environmental Science and Engineering, Fudan University, Shanghai, 200433, PR China

ARTICLE INFO

Article history:
Received 7 March 2020
Received in revised form
2 June 2020
Accepted 6 June 2020
Available online 11 June 2020

Keywords:
Cyanobacterial blooms
Phosphorus
Microcystin-LR
Biofilm
Extracellular polymeric substances

ABSTRACT

Cyanobacterial blooms cause potential risk to submerged macrophytes and biofilms in eutrophic environments. This pilot-scale study investigated the growth, oxidative responses, and detoxification activity of aquatic plants in response to cyanobacterial blooms under different phosphorus concentrations. Variations of extracellular polymeric substances (EPSs) and microbial community composition were also assessed. Results showed that the biomass of *Vallisneria natans* increased with exposure to cyanobacterial blooms at higher phosphorous concentrations ($P > 0.2$ mg L^{-1}). The amount of microcystin compounds (MC-LR) released into the water and the accumulation of MC-LR into both plant tissue and biofilms changed according to the phosphorus concentration. Furthermore, a certain degree of oxidative stress was induced in the plants, as evidenced by increased activity of superoxide dismutase, catalase, and peroxidase, as well as increased malondialdehyde concentrations; significant differences were also seen in acid phosphatase and glutathione S-transferase activities, as well as in glutathione concentrations. Together, these responses indicate potential mechanisms of MC-LR detoxification. Broader α-D-glucopyranose polysaccharides (PS) increased with increasing phosphorous and aggregated into clusters in biofilm EPS in response to the cyanobacterial blooms. In addition, alterations were seen in the abundance and structure of the microbial communities present in exposed biofilms. These results demonstrate that cyanobacterial blooms under different concentrations of phosphorus can induce differential responses, which can have a significant impact on aquatic ecosystems.

1. Introduction

Eutrophication is one of the serious issues facing global freshwater ecosystems, and results in the deterioration of lake and river environments (Smith and Schindler, 2009; Zhao et al., 2015). The frequency of cyanobacterial bloom outbreaks is one of the key consequences of eutrophication, representing a significant threat to both aquatic ecosystems and population health (Kumar et al., 2018). Phosphorus content in eutrophic water plays a vital role in the outbreak of cyanobacterial blooms, leading to low light environments and the production of harmful allelochemicals which results in species reduction and ecological deterioration (Xu et al., 2015). Increases in phosphorus at the sediment-water interface may influence the initiation of cyanobacterial blooms in lakes (Carey et al., 2009). During a cyanobacterial bloom, an undesirable smell is generated alongside a range of toxic compounds (Yin et al., 2005); among toxic compounds, microcystins (MCs) are the most common cyanotoxins of great ecological concern (Jiang et al., 2011). Controlling eutrophication and mitigating cyanobacteria is therefore necessary to help to prevent and control water pollution.

In recent years, cyanobacterial blooms frequently occurred in many large lakes and reservoirs in China, especially in Lake Taihu (Hu et al., 2016). Submerged macrophytes are an important part of the aquatic ecosystem and play a vital role in the purification of eutrophic water during cyanotoxin blooms (Wiegand and Pflugmacher, 2005). Despite this, the adverse aquatic environment generated by these blooms also has harmful effects on these plants. Previous studies confirmed that MCs released in water can directly contact plants and inhibit their growth rate and germination, and can trigger oxidative stress by promoting the release of reactive oxygen species (ROS) (Leflaive and Ten-Hage, 2007). MC-LR has been demonstrated to be taken up by *Ceratophyllum demersum*, *Elodea canadensis*, *Vesicularia dubyana,* and *Vallisneria natans,* influencing their germination, development, and photosynthesis (Pflugmacher, 2002, 2004; Pflugmacher et al., 1998). Due to the many negative impacts that it can have, investigation into the

* Corresponding author.
E-mail address: zzhenghj@fudan.edu.cn (Z. Zheng).

https://doi.org/10.1016/j.envpol.2020.114996
0269-7491/

effects of MC-LR on aquatic plants is crucial for understanding eutrophic aquatic ecosystem restoration. In addition, as phosphorous is critical to eutrophication and is closely related to cyanobacterial blooms, its influences on cyanobacterial toxicity are of importance; however, studies on the effects of cyanobacterial blooms on submerged macrophytes in terms of the influence of phosphorus concentration are rare.

In natural aquatic ecosystems, biofilms comprised of complex microbial communities are formed on the natural substrates of submerged macrophytes; these biofilm communities can cooperate with the plants to regulate aquatic ecological functions and aid in survival (Zhao et al., 2018). Previous studies have shown that biofilms play vital roles in the food chain, in modulating nutrient cycles, and in eutrophic water restoration (Liu et al., 2016). In particular, the biofilms of submerged macrophytes are regarded as the front line for interactions between pollutants and plant tissues; periphytic biofilms play an especially critical role in phosphorous cycling in aquatic environments due to their high affinity for phosphorus (Drake et al., 2012). Because of their importance, it is necessary to investigate the changes that occur in biofilms in response to cyanobacterial blooms under different phosphorus loadings.

As an important microbial aggregate in the aquatic system, biofilms have complicated structures containing an abundance of cells; these structures are primarily constructed with a matrix of extracellular polymeric substances (EPS) (Flemming and Wingender, 2010). As the primary materials composing EPS, polysaccharides (PS), proteins, and other macromolecules have the ability to sustain the biofilm mechanical stability. Cyanobacterial blooms in eutrophic lakes can induce adverse effects on biofilms, and interactions under different P loadings can induce complex changes in the biofilms which also alter the physicochemical characteristics of the associated EPS (Shrout and Nerenberg, 2012).

This pilot-scale study aimed to comprehensively investigate the effects of cyanobacterial blooms on *Vallisneria natans* and on biofilms at different phosphorus concentrations. Specifically, plant growth and antioxidant system metabolites were examined, and the contents of MC-LR in plants and biofilms as well as their detoxification metabolites were studied. EPS spatial distribution and microbial properties were also examined in biofilms, in order to better understand the potential impacts the blooms may have on eutrophic environments.

2. Materials and methods

2.1. Cultivation of V. natans and set up of pilot-scale system

V. natans plants were purchased from the Tiancun Horticultural Company (Shanghai, China) and grown in a 1/10 Hoagland solution. All plants were cultivated for 7 days, after which green and healthy plants were selected and cleaned prior to subsequent experiments. A total of 30.0 g of fresh weight (FW) plants were cultivated in a pond with 800 L water and 50 mm of silica sand (ADA aqua soil, Aqua Design Amano Company, Japan). Each pond covered 1 m^2 (1.0 m length x 1.0 m width x 1.0 m high) with a volume of 1 m^3. Water was obtained from Lake Taihu (location coordinates:120.1, 31.5, China) which contained the cyanobacterial population. Before the experiment, all treatments were standardized to contain 1.92×10^8 cyanobacterial cells L^{-1}. The range of cyanobacterial cell densities throughout the experiment was measured to be 1.92-5.69 $\times$ 10^8 cyanobacterial cells L^{-1}. Phosphorus stock solutions were added to different containers to maintain constant concentrations of 0, 0.05, 0.10, 0.20, 0.50 and 1.00 mg L^{-1} for 30 days. All containers were placed near the lake to keep the same environment as the lake water. All of the experiments took place during summer (with a mean monthly air temperature of 20−30 °C). Each treatment was performed in triplicate. Water samples in containers were collected for MC-LR analysis. Plants were also sampled at 0, 10, and 30 days to assess their biomass as well as concentrations of some chemicals and analysis of enzyme activity. Periphyton biofilms were collected to analyze microbial community composition at the end of the experiment.

2.2. Plant growth, enzyme activity, and metabolite assays

To analyze the growth of *V. natans*, the fresh weights (FW) along with shoots and root length of samples were tested after 30 days, and biomass was calculated using plant density (g FW m^{-2}). To assess the enzyme activity of *V. natans*, 1.0 g FW plants were frozen with liquid nitrogen and then ground with 10 mL 0.1 mol L^{-1} phosphate buffer (PBS, pH 7.0). The resulting homogenate was centrifuged at 10,000×*g* at 4 °C for 20 min to collect supernatants. The activities of superoxide dismutase (SOD), peroxidase (POD), catalase (CAT), acid phosphatase (ACP), and glutathione S-transferase (GST) were tested from supernatants following the manufacturer's instructions from the respective commercialized chemical assay kits (Nanjing Jiancheng Bioengineering Institute, China), along with the malondialdehyde (MDA) and glutathione (GSH) content.

2.3. MC-LR analysis

To determine MC-LR content, a 10 mL water sample was vacuum filtered through microfiber filters (42 mm, 0.45 μ, Whatman, England) for further analysis. To test the MC-LR concentration in both plants and biofilms, 1.0 g (FW) plant sample with biofilm material was frozen, crushed, and blended with 10 mL 0.1 mol L^{-1} PBS (pH 7.0). After centrifuging the homogenate (4000×*g* for 20 min), the supernatant was collected and filtered through a glass-fiber filter (0.45 μ) (Kumar et al., 2018). The contents were tested for MC-LR using an MC-LR enzyme-linked immunosorbent assay (ELISA) kit (Mlbio Company, China). All processing operations were performed at 4 °C and each sample was analyzed in triplicate.

2.4. Multiple fluorescent staining

Confocal laser scanning microscopy (CLSM) and multiple fluorescent staining were used to visualize the spatial distribution of protein as well as both α- and β-D-glucopyranose PS in biofilms and leaves. After 30 days, the plant leaves with biofilms were collected and fixed with 2.5% glutaraldehyde for 24 h in a dark environment. All samples were then stained with 50 μL of 1 g L^{-1} fluorescein-isothiocyanate (FITC) (Sigma, St. Louis, MO, USA) for 1 h at room temperature, followed by the addition 100 μL of 250 mg L^{-1} concanavalin A (Con A) (Sigma) for 30 min; Following this, 100 μL of 300 mg L^{-1} calcofluor white (CW) (Sigma) was added and samples were incubated for another 30 min. Samples were then washed with PBS to remove excess stain. Finally, a CLSM (LEICA SP8, Germany) was used to observe the internal structure of stained samples. The excitation/emission wavelengths that were used to observe FITC, Con A, and CW were 488/520 (green), 552/580 (red), and 405/435 nm (blue), respectively (Adav et al., 2010; Chen et al., 2007).

2.5. Microbe examination

At the end of the experiment, 1.0 g FW samples (leaves with biofilms) were harvested and kept in 20 mL 0.1 mol L^{-1} PBS solution. The mixture was ultrasonicated for 1 min to obtain suspensions containing the microbes from the biofilms. The suspensions

were shaken for 5 min at room temperature and centrifuged at 10,000×*g* for 5 min. Sediments were collected and stored at −80 °C for further DNA isolation and examination. The E.Z.N.A. Soil DNA Kit (Omega, D5625-01, USA) was used for extraction of microbial DNA, and high-throughput sequencing was conducted by Majorbio Bio-Pharm Technology Co., Ltd. (Shanghai, China) on an Illumina MiSeq platform. After obtaining results, the sequences were analyzed to obtain the diversity of microbial communities and identification of microbial species. The bacterial community structure and abundance of biofilms on *V. natans* leaves were assessed using the online platform Majorbio I-Sanger Cloud Platform (www.i-sanger.com).

2.6. Statistical analysis

GraphPad Prism software was used to process all data, while data was analyzed using SPSS software (Version 22.0, SPSS Inc., Chicago, IL, USA). Comparisons between different samples were performed by two-way analysis of variance (ANOVA) and significant differences were determined by *LSD* (Least Significant Difference) tests. Each experiment was performed in triplicate and statistical significance was determined at $p < 0.05$. Redundancy analysis (RDA) was performed using CANOCO 5.0 software (Ithaca, NY, USA) to determine the relationships between antioxidant biochemical responses and environmental parameters.

3. Results and discussion

3.1. Plant growth

The effects of different phosphorus concentrations on the growth of *V. natans* were shown in Fig. 1. Higher phosphorus concentrations (P > 0.2 mg L^{-1}) promoted plant growth when compared with the control group, though biomass decreased with increasing concentrations of phosphorus (P > 0.2 mg L^{-1}). The highest biomass and shoot length was observed at 0.2 mg L^{-1} P, indicating that *V. natans* can growth well at this concentration (Fig. 1b). Previous studies have demonstrated that submerged macrophytes could absorbed the phosphorus through both roots and shoots (Rattray et al., 1991); low concentration of nutrients promoted the accumulation of *V. natans* biomass while higher nutrient concentrations had the opposite effects (Wen et al., 2008). In addition, a related study has confirmed that submerged macrophytes grow better when phosphorous concentrations were less than 0.2 mg L^{-1}. When the TP concentration was greater than 0.4 mg L^{-1}, submerged plants suffered more stress and growth inhibition, with increasing stress correlating with increasing concentrations of phosphorus (Tang, 2019). In this study, it was found that a low content of phosphorous promoted the accumulation of biomass, as longer root length was observed in control group, where *V. natans* generated longer roots to absorb more nutrients. This lower biomass also makes sense in terms of cyanobacterial enrichment, as higher phosphorous would result in an increase of cyanobacterial blooms, decreasing the growth of *V. natans* due to the presence of secondary metabolites from the cyanobacteria (Przytulska et al., 2017; Wang et al., 2017).

3.2. Oxidative response

After one month, the oxidative stress response of *V. natans* to cyanobacterial blooms was investigated under different phosphorus concentrations (Fig. 2). As the final product of lipid peroxidation, MDA content is positively correlated with the content of ROS (Chao et al., 2008). Two-way ANOVA indicated that there was no significant interaction with MDA across the different

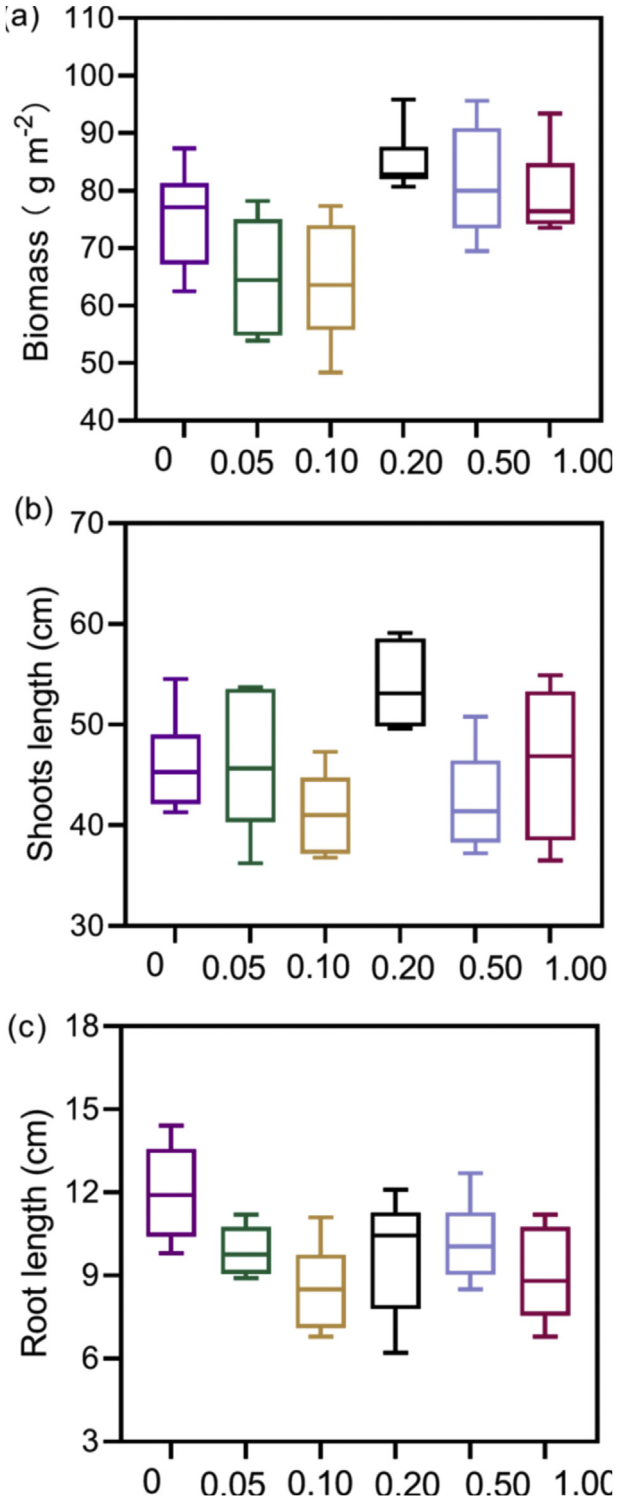

Fig. 1. Changes of the biomass (a), shoot length (b) and root length (c) of *Vallisneria natans* leaves in the experimental period.

phosphorus treatments after 10 days (Fig. 2a). At the end of the experiment (day 30), the MDA content of plants under low phosphorous conditions increased in comparison to the control; at higher phosphorous concentrations (P > 0.5 mg L^{-1}), MDA content decreased in comparison to the control. The highest MDA content was observed at P = 0.1 mg L^{-1}. A low concentration of P is beneficial to the growth of plants and algae, and previous study also

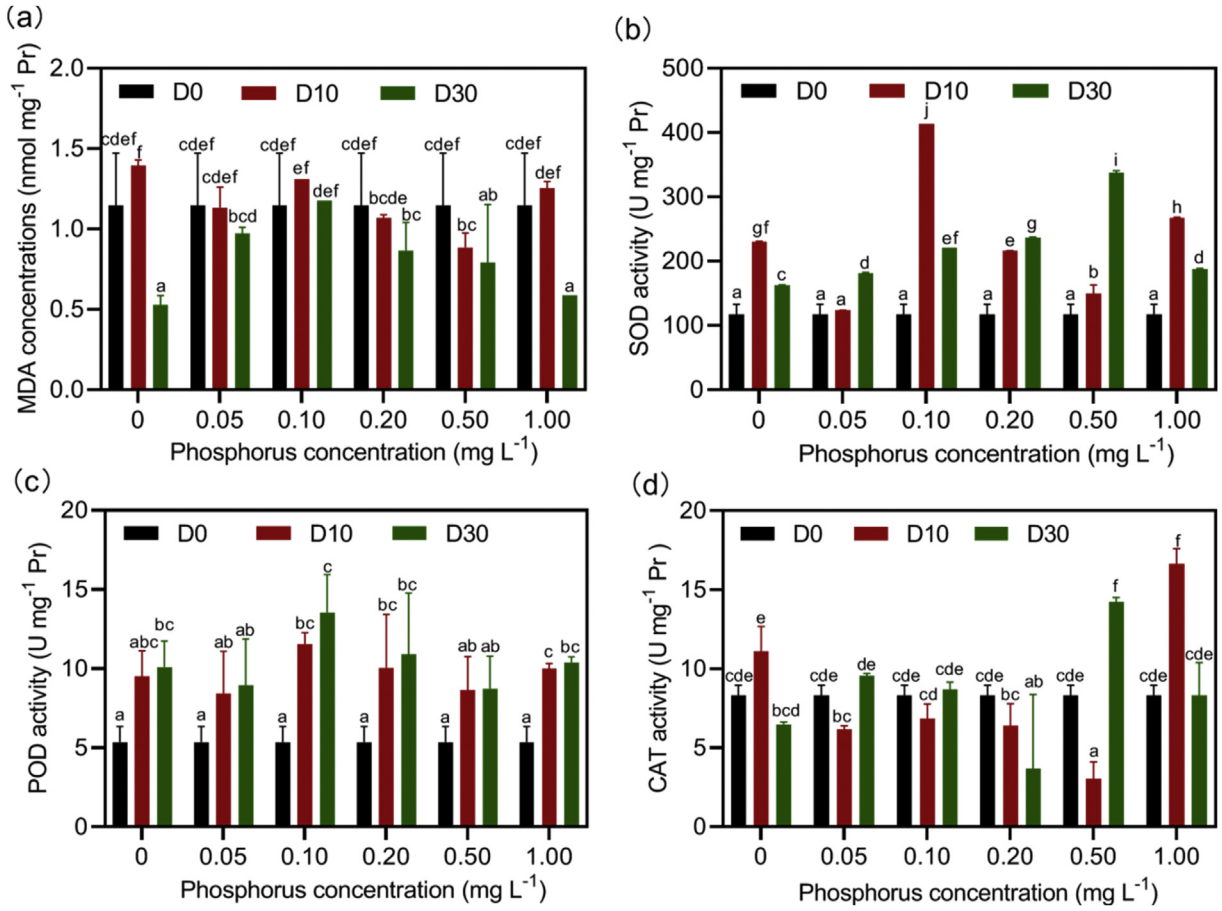

Fig. 2. The change of MDA content (a) and antioxidant system (b–d) of *V. natans* leaves. Data are means ± standard deviation analyzed from three replicates. Different letters (a–j) indicate significant difference ($p < 0.05$). D0: Day 10, D10: Day 10, D30: Day 30.

confirmed the 0.1 mg L^{-1} P was suitable for algae grown (V.H. Smith et al., 1999). Meanwhile, more MCLR which released from the more algae will enters the plant cell with the low concentration P treatment (Fig. 3b) and caused more oxidative stress (increased MDA in Fig. 2). At higher phosphorus concentrations (P > 0.2 mg L^{-1}), MCLR content decreased in plant (Fig. 3b). Tang (2019) also confirmed the P became a plant stress factor, as well as the MCLR. Previous study has confirmed that the plants will absorb MC and subsequently develop an antioxidant system when the MC-LR > 1.09 ng g^{-1} of plant tissue (Jiang et al., 2011). Therefore, we assumed the increased MDA content caused by MC which absorbed by plant in cyanobacterial blooms, and the variations in MDA level also weakly negative related to different phosphorous conditions (Fig. 3c). Previous studies have also shown that the production of superoxide was significantly increased in plants exposed to MC (Jiang et al., 2011). This result indicates that oxidative stress occurred in *V. natans* during exposure to cyanobacterial blooms; this correlates with previous research indicating there is a close relationship between cyanobacterial bloom outbreaks and phosphorus concentration (Zhu et al., 2008).

During the experiment, SOD activity of plants treated with phosphorus were higher than control group, with the highest value observed at P = 0.1 mg L^{-1} in the 10 day samples (Fig. 2b). At the end of the treatment, the values of SOD increased with enhanced phosphorus concentration, but then decreased at 1.00 mg P L^{-1}. A similar trend was observed with POD activity when compared to the control group (Fig. 2c); the highest values were also seen at 0.1 mg P L^{-1} in 10 day and 30 day samples, which were also significantly higher than initial measurements. No notable changes were observed in CAT activity with low P exposure (P < 0.2 mg L^{-1}), however higher CAT activity was seen in plants under higher P concentration exposure (Fig. 2d). An abundance of reports show that reactive oxygen species (ROS) are induced in plants in response to adverse environments stress, and that CAT, SOD, and POD enzymes play a vital role in ROS scavenging to preventing oxidative damage to cells (Fridovich, 2013; Gueta-Dahan et al., 1997). It is therefore reasonable to assume that CAT, POD, and SOD may also be involved in the protective process against oxidative stress induced by MC-LR generated from the cyanobacteria in eutrophic lakes (Wang and Wang, 2018). Overall, these results demonstrate that cyanobacterial blooms with different phosphorus loadings cause a certain degree of oxidative stress on *V. natans*.

3.3. Uptake of MC-LR by V. natans and the detoxification pathway

To investigate the effects of cyanobacterial blooms on submerged macrophytes under different phosphorus loadings, the content of MC-LR in water along with the amount accumulated in leaves and biofilms were tested (Fig. 3). MC-LR is the toxin most frequently produced by freshwater cyanobacteria. The amounts of MC-LR released to the aquatic environment from the cyanobacteria were sustained during the 30 day period. After 10 days of treatment, the content of MC-LR significantly increased in the water (Fig. 3a); the highest value was observed at 1.0 mg P L^{-1}, while no significant difference was seen under other treatment conditions. At the end of the experiment, there were no significant differences

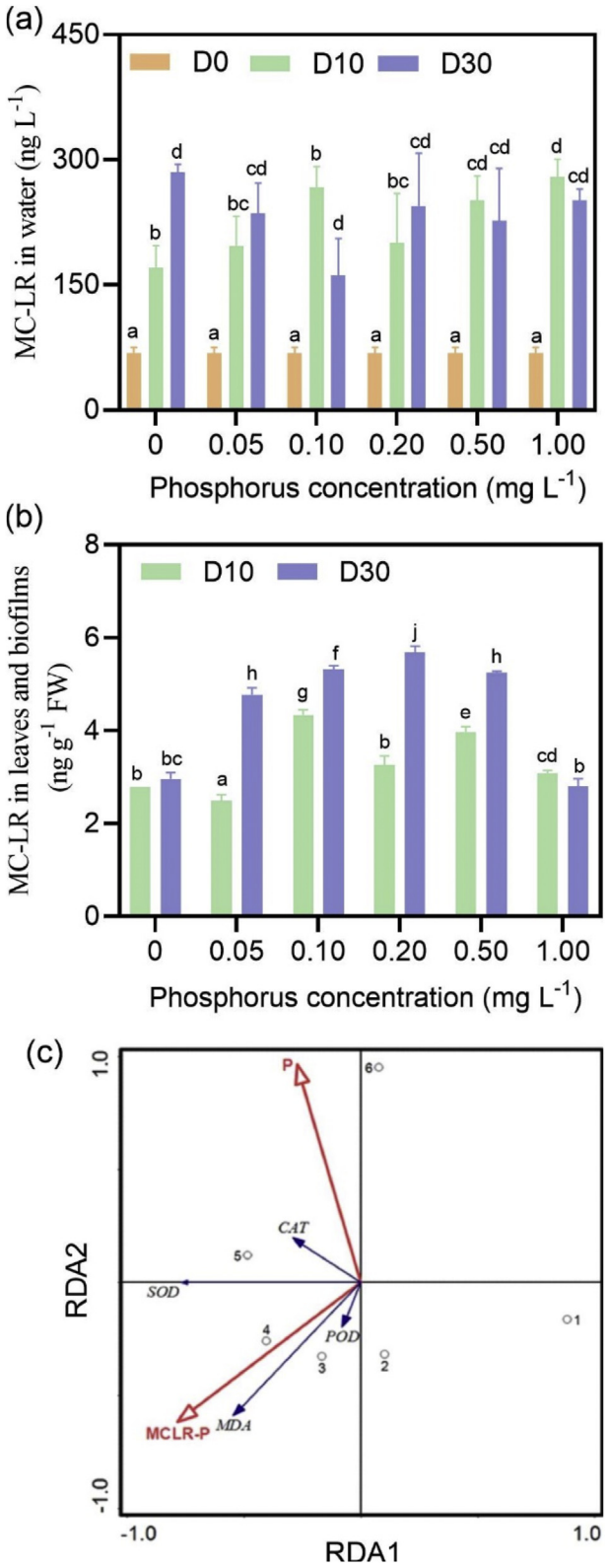

Fig. 3. The content of MC-LR in water body (a), plant leaves and biofilms (b) during 30 days and redundancy analysis (RDA) diagram of the relation between antioxidant biochemical responses and environmental parameters (c). Different letters (a–i) indicate significant difference ($p < 0.05$). D0: Day 10, D10: Day 10, D30: Day 30. P: phosphorus concentration, MCLR-P: MCLR in leaves.

observed between the various P treatments. Previous studies have shown that submerged macrophytes could allelopathically be affected by cyanobacteria extracts and excreted compounds during the exponential and decline phase (Xu et al., 2015; Zheng et al., 2013). In addition, Fig. 3b shows that the maximum uptake of MCLR after 30 days was 5.68 ng g^{-1} FW in plant tissue and biofilms when exposed to 0.20 mg L^{-1} phosphorus treatment. The final levels of MCLR in plants were higher than that measured after 10 days, indicating the plants were taking up MC-LR throughout the full treatment period. Besides, RDA analysis results showed that different environmental parameters were positively or negatively correlated with the MDA content and antioxidant enzyme in different treatment (Fig. 3c). Generally, the phosphorus content correlated weakly negatively with MDA content and POD activities with the slightly obtuse angle. Meanwhile, the MC-LR in plants correlated positively with antioxidant enzyme and MDA content particularly. However, the angle between MCLR in plants and phosphorus content is close to the right angle, which means weakly relationship. Previous studies have shown that MC-LR can be taken up by aquatic plants, but that concentrations absorbed reached a plateau after 14 days (Jiang et al., 2011); phosphorus enrichment of water has also been shown to promote the release of cyanobacterial pigments (Przytulska et al.). The results of this experiment indicate that the released MC-LR from the cyanobacterial bloom changed under different phosphorus concentrations, and that its accumulation in plant tissue was weakly related to the phosphorus concentration in the surrounding aquatic environment.

As shown in Fig. 4a, the activity of acid phosphatase was decreased under exposure to different phosphorus concentrations during 30 days of treatment. The ACP activity gradually increased in the lower phosphorus treatments, but decreased at higher phosphorus concentrations. Phosphorus absorption by many plants involves enhanced expression and secretion of ACP (Miller et al., 2001). Previous studies have reported that the activity of ACP in plants was significantly increased by low phosphorus treatment, but inhibited by high phosphorus (Weiwei Wang and Zhao., 2017; Zhang, 2014). This study confirmed that the submerged macrophytes show a similar pattern of ACP activity in response to different phosphorus treatments. The potential detoxification mechanisms of MC-LR in plant leaves are presented in Fig. 4b. Significant differences in GST activity and GSH concentrations of plant tissue were observed when exposed to cyanobacterial blooms with different phosphorus loadings; higher GSH content was observed at 0.1 and 0.2 mg P L^{-1} when tissue was examined at the end of the experiment. Higher amounts of MC-LR accumulation in plant tissue was also observed under these treatment conditions (Fig. 3b). A specific amount of MC-LR can be removed by enzymatic conjugation to GSH though the GST system in plant cells(P-flugmacher, 2002). Following this, the GSH conjugate in the cytosol is removed to the vacuole by special proteins for storage and further processing (Coleman et al., 1997). The initial increase of GSH concentration observed in this experiment was likely due to the GSH generation induced by low MC-LR content uptake, which decreased later with the formation of the glutathione conjugate (Jiang et al., 2011; Stephan et al., 2007; Stüven and Pflugmacher, 2007).

3.4. EPS characteristics and microbial properties in biofilms

3.4.1. EPS characteristics

To visualize the varied properties of key organic compounds in biofilms as they responded to cyanobacterial blooms at different phosphorus concentrations, the triple staining CLSM technique was used, and the protein, α-, and β-D-glucopyranose polysaccharides (PS) in biofilms from each treatment condition were observed. As

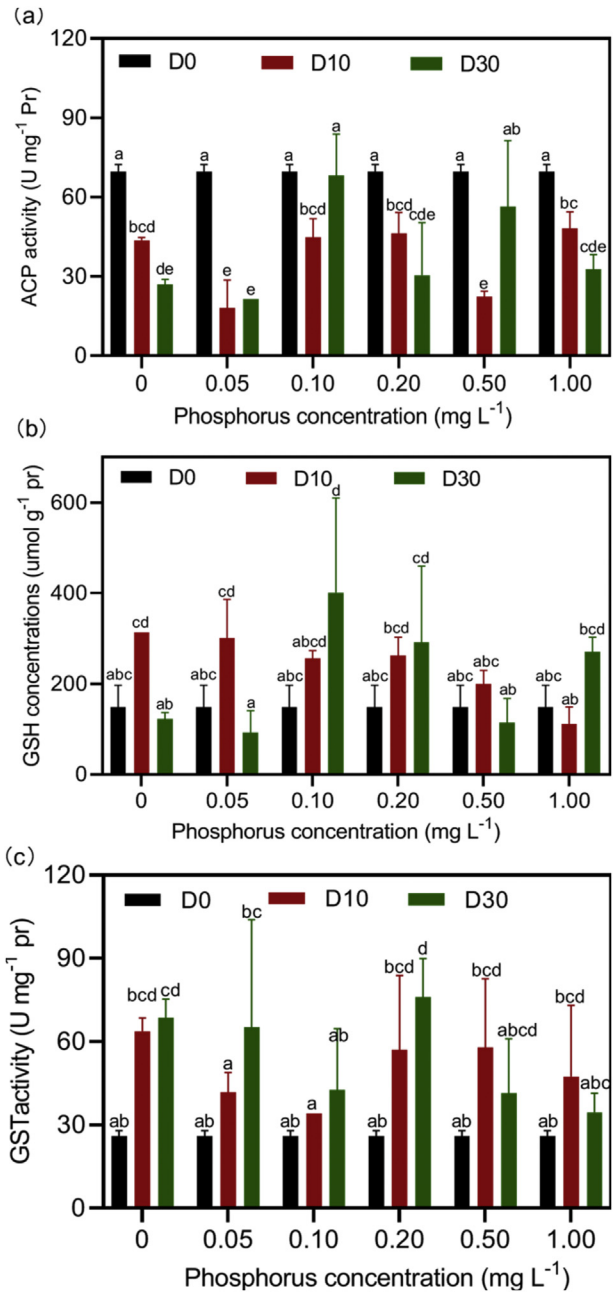

Fig. 4. The change of ACP activity (a), GSH concentrations (b) and GST activity (c) of *V. natans* leaves. Data are means ± standard deviation analyzed from three replicates. Different letters (a–f) indicate significant difference ($p < 0.05$). D0: Day 10, D10: Day 10, D30: Day 30.

shown in Fig. 5, the α-D-glucopyranose PS (red) was the dominant compound, and aggregated into clusters in the biofilms. Higher amounts of α-D-glucopyranose PS were found with increasing concentrations of phosphorus. Little β-D-glucopyranose PS (blue) was found with phosphorus treatment (Fig. 5d), and the highest density of α-D-glucopyranose PS and β-D-glucopyranose PS was observed in the highest concentration of phosphorus. Although the α- and β-D-glucopyranose PS were non-homogeneously distributed across the depth of the biofilms, PS plays an important role in keeping the structural integrity of the biofilm matrix (Lux et al., 2005). Previous research has also shown a broader distribution of a-D-glucopyranose polysaccharides (PS), and demonstrated that increased production and broader distribution of b-D-glucopyranose PS can create a formidable shield in response to exposure to harmful chemicals (Wang et al., 2018). Thus, alteration in the functional characteristics and spatial structure of biofilms are vital indicators for the response of biofilms to the presence of cyanobacterial blooms with different phosphorus concentrations.

3.4.2. Microbial properties in biofilms

To further investigate the response of the microbial community in the biofilms to differential phosphorous concentrations, the abundances and structures of leaf biofilms were examined using 16 S rRNA sequencing (Fig. 5). *Proteobacteria, Cyanobacteria, Bacteroidetes,* and *Acidobacteria* were the dominant phyla identified in all samples (Fig. 5c), and all have previously been reported to be present in leaf biofilms of aquatic plants (Gong et al., 2018). Previous reports showed that *Proteobacteria* were the dominant microorganisms observed in shallow lake biofilms, and that these bacteria are widely distributed (Liu et al., 2009). These predominant species contributed to the stability of biofilms with their metabolic functions and EPS secretions (Lv et al., 2014). A genus of *Proteobacteria*, *Rhodocyclus,* is able to perform polyphosphate accumulation in aquatic environments(Carr et al., 2003). In order to further determine the community structure in the biofilms, further analysis of microbial community composition was performed at the genus level (Fig. 6a). Here, hierarchical clustering analysis indicated that the cyanobacteria blooms with different phosphorus concentrations changed the structure of the microbial community of the biofilms, and different phosphorous treatments affected the epiphytic microbial diversity. Previous study has indicated that cyanobacterial blooms in the decline phase can release a higher amount of MC-LR, which exerts notable change in the microbial diversity of biofilms (Li et al., 2019). Venn diagrams presenting the distribution of operational taxonomic units (OTU) in biofilms, are used to show the common and unique microbial community members between different samples (Schloss et al., 2013). As shown in Fig. 6b, the unique OTUs found in the different treatments were 625 (P1), 1163 (P2), 1213 (P3), 1547 (P4), 1278 (P5) and 639 (P6), indicating that different phosphorus concentrations had notable effects on altering the microbial diversity of biofilms in water containing cyanobacterial blooms.

4. Conclusions

This pilot-scale experiment investigated the effects of cyanobacterial blooms on submerged macrophytes and biofilms under different phosphorus concentrations. Results demonstrate that *V. natans* growth was differentially affected by the cyanobacterial blooms under different phosphorus conditions. A certain degree of oxidative stress was found to be induced in *V. natans*, as indicated by increased activities of CAT, SOD, POD, as well as increased MDA concentrations. Furthermore, this study found that the amount of MC-LR released by the cyanobacterial blooms changed under different phosphorus concentrations, and that its accumulation in plant tissue was weakly related to the phosphorus concentration in the surrounding aquatic environment. Significant differences in GST activity and GSH concentrations in the plants were observed, indicating the potential detoxification mechanisms of MC-LR in plant leaves and biofilms. Moreover, larger changes occurred in EPS spatial distribution in response to cyanobacterial blooms under increased phosphorous concentrations, where increased amounts of α-D-glucopyranose PS were observed. Alteration of the abundances and structure of the microbial community in the biofilms

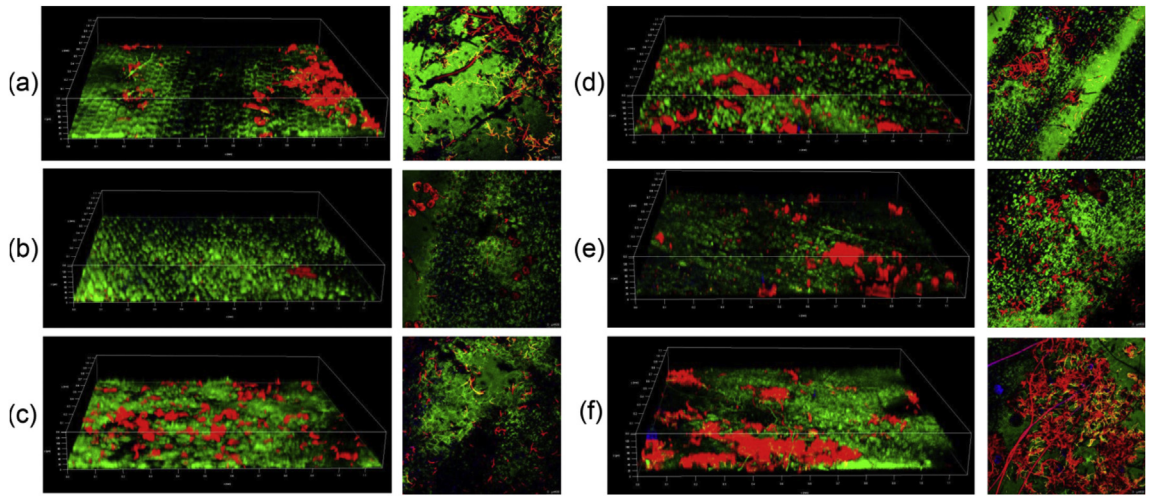

Fig. 5. Effects of phosphorus content on EPS spatial distribution in biofilms. The left column is the 3-D projection, and the right side represents the 2-D images of the top layer in each sample (a: control group; b: 0.05 mg L^{-1}; c: 0.1 mg L^{-1}; d: 0.2 mg L^{-1}; e: 0.5 mg L^{-1} and f: 1.0 mg L^{-1}). Biofilms were stained with FITC (proteins in green), Con A (a-D-glucopyranose polysaccharides in red) and CW (b-D-glucopyranose polysaccharides in blue). The bar in the 2-D images is 100 μm long. (For interpretation of the references to colour in this figure legend, the reader is referred to the Web version of this article.)

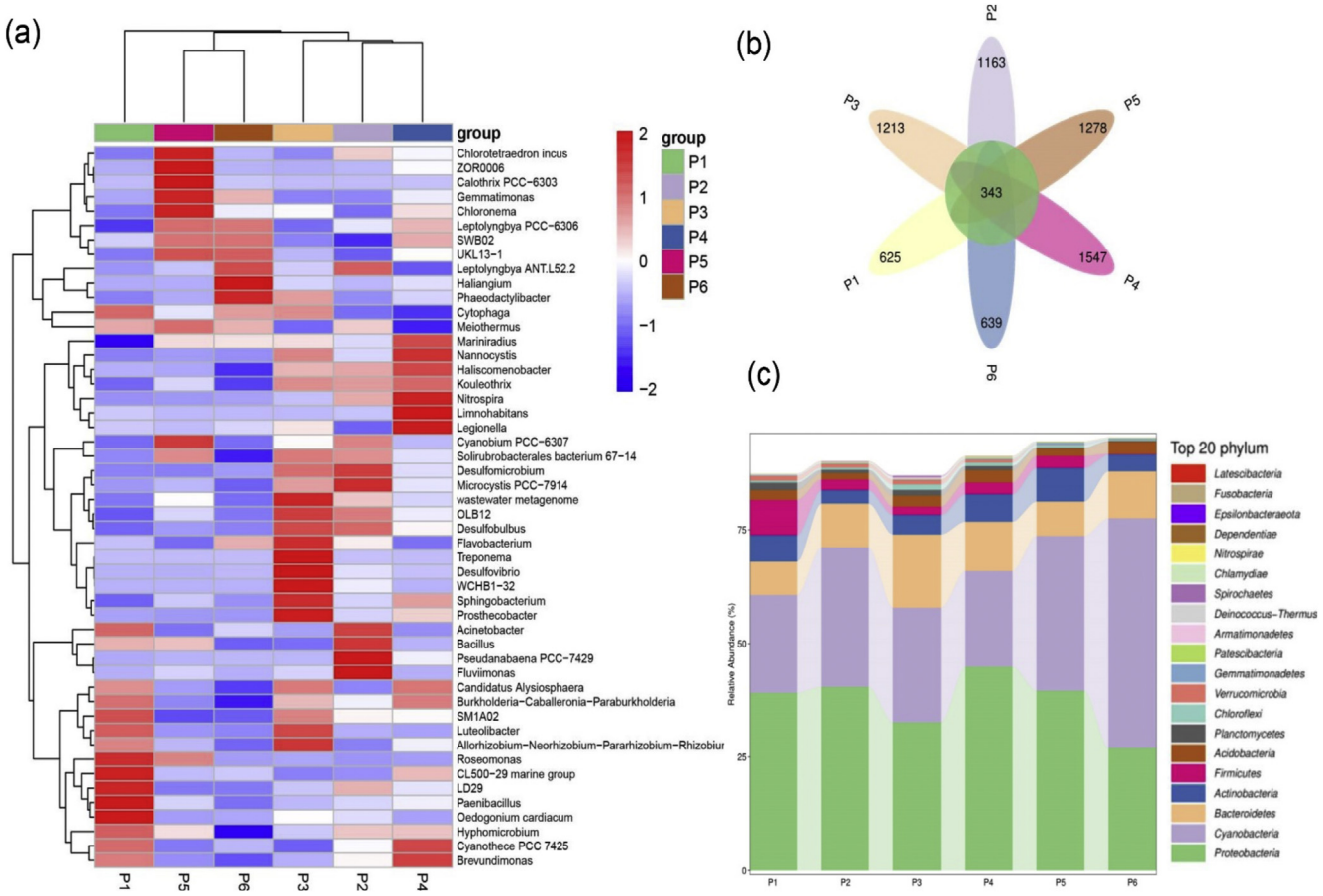

Fig. 6. Microbial community analysis: (a) heat-map of the different samples at the genus level, (b) Venn diagram of distribution of OTUs in different samples and (c) Bar chart of the different samples at the phylum level in different samples. P1: control group; P2: biofilms in phosphorus with concentration 0.05 mg L-1; P3: 0.1 mg L-1; P4: 0.2 mg L-1; P5: 0.5 mg L-1 and P6: 1.0 mg L-1.

were also seen to differ based on the concentration of phosphorous present. These results provide valuable information on the ecological effects of cyanobacterial blooms on submerged macrophytes and periphyton biofilms under different phosphorus

concentrations.

CRediT authorship contribution statement

Qi Li: Conceptualization, Data curation, Writing - original draft, Software. **Peng Gu:** Investigation, Resources. **Xin Luo:** Writing - review & editing. **Hao Zhang:** Data curation. **Suzhen Huang:** Writing - review & editing. **Jibiao Zhang:** Conceptualization, Methodology. **Zheng Zheng:** Supervision.

Declaration of competing interest

The authors declare that they have no known competing financial interests or personal relationships that could have appeared to influence the work reported in this paper.

Acknowledgments

This work was supported by the Major Science and Technology Program for Water Pollution Control and Treatment (2017ZX07204005, 2012ZX07103004) and ABA Chemicals.

Appendix A. Supplementary data

Supplementary data to this article can be found online at https://doi.org/10.1016/j.envpol.2020.114996.

References

Adav, S.S., Lin, J.C.T., Yang, Z., Whiteley, C.G., Lee, D.J., Peng, X.F., Zhang, Z.P., 2010. Stereological assessment of extracellular polymeric substances, exo-enzymes, and specific bacterial strains in bioaggregates using fluorescence experiments. Biotechnol. Adv. 2**8** (2), 255–280.

Carey, C.C., Weathers, K.C., Cottingham, K.L., 2009. Increases in phosphorus at the sediment-water interface may influence the initiation of cyanobacterial blooms in an oligotrophic lake. Int. Ass. Theor. Appl. Limnol. 30 (8), 1185–1188.

Carr, E.L., Bkc, K.P., Gurtler, V., Seviour, R.J., 2003. Seven novel species of Acinetobacter isolated from activated sludge. Int. J. Syst. Evol. Microbiol. 53 (4), 953–963.

Chao, W., Zhang, S.H., Wang, P.F., Hou, J., Li, W., Zhang, W.J., 2008. Metabolic adaptations to ammonia-induced oxidative stress in leaves of the submerged macrophyte *Vallisneria natans (Lour.)*. Hara. Aquat. Toxicol. 87 (2), 88–98.

Chen, M.Y., Lee, D.J., Tay, J.H., Show, K.Y., 2007. Staining of extracellular polymeric substances and cells in bioaggregates. Appl. Microbiol. Biotechnol. 75 (2), 467–474.

Coleman, J., Blake-Kalff, M., Davies, E., 1997. Detoxification of xenobiotics by plants: chemical modification and vacuolar compartmentation. Trends Plant Sci. 2 (4), 144–151.

Drake, W.M., Scott, J.T., Evans-White, M., Haggard, B., Sharpley, A., Rogers, C.W., Grantz, E.M., 2012. The effect of periphyton stoichiometry and light on biological phosphorus immobilization and release in streams. Limnology 13 (1), 97–106.

Flemming, H.C., Wingender, J., 2010. The biofilm matrix. Nat. Rev. Microbiol. 8 (9), 623–633.

Fridovich, I., 2013. Superoxide dismutase. Adv. Enzymol. Relat. Area Mol. Biol. 58, 352–354.

Gong, L., Zhang, S., Chen, D., Liu, K., Lu, J., 2018. Response of biofilms-leaves of two submerged macrophytes to high ammonium. Chemosphere 192, 152–160.

Gueta-Dahan, Y., Yaniv, Z., Zilinskas, B.A., Ben-Hayyim, G., 1997. Salt and oxidative stress: similar and specific responses and their relation to salt tolerance in Citrus. Planta 203 (4), 460–469.

Hu, L., Kun, S., Lizhou, L., Wei, S., Licheng, H., Nanqin, G., Lirong, S., 2016. Multi-year assessment of toxic genotypes and microcystin concentration in northern Lake Taihu, China. Toxins 8 (1), 23.

Jiang, J., Gu, X., Song, R., Wang, X., Yang, L., 2011. Microcystin-LR induced oxidative stress and ultrastructural alterations in mesophyll cells of submerged macrophyte *Vallisneria natans (Lour.) Hara*. J. Hazard Mater. 190 (1–3), 188–196.

Kumar, P., Hegde, K., Brar, S.K., Cledon, M., Kermanshahi-Pour, A., Roy-Lachapelle, A., Galvez-Cloutier, R., 2018. Biodegradation of microcystin-LR using acclimatized bacteria isolated from different units of the drinking water treatment plant. Environ. Pollut. 242 (Pt A), 407–416.

Leflaive, J., Ten-Hage, L., 2007. Algal and cyanobacterial secondary metabolites in freshwaters: a comparison of allelopathic compounds and toxins. Freshw. Biol. 52, 199–214.

Li, Q., Gu, P., Zhang, H., Luo, X., Zhang, J., Zheng, Z., 2019. Response of submerged macrophytes and leaf biofilms to the decline phase of Microcystis aeruginosa: antioxidant response, ultrastructure, microbial properties, and potential mechanism. Sci. Total Environ. 134325.

Liu, Y., Yao, T., Zhu, L., Jiao, N., Liu, X., Zeng, Y., Jiang, H., 2009. Bacterial diversity of freshwater alpine lake puma yumco on the Tibetan plateau. Geomicrobiol. J. 2**6** (2), 131–145.

Liu, J., Liu, W., Wang, F., Kerr, P., 2016. Redox zones stratification and the microbial community characteristics in a periphyton bioreactor. Bioresour. Technol. 204, 114–121.

Lux, R., Li, Y., Lu, A., Shi, W., 2005. Detailed three-dimensional analysis of structural features of Myxococcus xanthus fruiting bodies using confocal laser scanning microscopy. Biofilms 1 (4), 293–303.

Lv, Y., Wan, C., Lee, D.J., Liu, X., Tay, J.H., 2014. Microbial communities of aerobic granules: granulation mechanisms. Bioresour. Technol. 169, 344e351.

Miller, S.S., Liu, J.Q., Allan, D.L., Menzhuber, C.J., Vance, C.P., 2001. Molecular control of acid phosphatase secretion into the rhizosphere of proteoid roots from phosphorus-stressed white lupin. Plant Physiol. 127 (2), 594–606.

Pflugmacher, S., 2002b. Possible allelopathic effects of cyanotoxins, with reference to microcystin-LR, in aquatic ecosystems. Environ. Toxicol. 17 (4), 407–413.

Pflugmacher, S., 2004. Promotion of oxidative stress in the aquatic macrophyte Ceratophyllum demersum during biotransformation of the cyanobacterial toxin microcystin-LR. Aquat. Toxicol. 70 (3), 169–178.

Pflugmacher, S., Wiegand, C., Oberemm, A., Beattie, K.A., Steinberg, C.E.W., 1998. Identification of an enzymatically formed glutathione conjugate of the cyanobacterial hepatotoxin microcystin-LR: the first step of detoxication. Biochim. Biophys. Acta 1425 (3), 527–533.

Przytulska, A., Bartosiewicz, M., Vincent, W.F., 2017. Increased risk of cyanobacterial blooms in northern high-latitude lakes through climate warming and phosphorus enrichment. Freshw. Biol. 62 (12), 1986–1996.

Rattray, M.R., Howard Williams, C., Brown, J.M.A., 1991. Sediment and water as sources of nitrogen and phosphorus for submerged rooted aquatic macrophytes. Aquat. Bot. 4**0** (3), 225–237.

Schloss, P.D., Dirk, G., Westcott, S.L., 2013. Reducing the effects of PCR amplification and sequencing artifacts on 16S rRNA-based studies. PloS One 6 (12), e27310.

Shrout, J.D., Nerenberg, R., 2012. Monitoring bacterial twitter: does quorum sensing determine the behavior of water and wastewater treatment biofilms? Environ. Sci. Technol. 46 (4), 1995–2005.

Smith, V.H., Schindler, D.W., 2009. Eutrophication science: where do we go from here? Trends Ecol. Evol. 24 (4), 201–207.

Smith, V.H., G D T, Nekola, J.C., 1999. Eutrophication impacts of excess nutrient inputs on freshwater, marine and terrestrial ecosystems. Environ. Pollut. 100 (3), 179–197.

Stephan, P., Marika, A., Bernhard, G., 2007. Influence of a cyanobacterial crude extract containing microcystin-LR on the physiology and antioxidative defence systems of different spinach variants. New Phytol. 175 (3), 482–489.

Stüven, J., Pflugmacher, S., 2007. Antioxidative stress response of *Lepidium sativum* due to exposure to cyanobacterial secondary metabolites. Toxic. Off. J. Int. Soc. Toxinol. 50 (1), 85–93.

Tang, Z., 2019. Study on the Tolerance of Three Submerged Plants to Nitrogen and Phosphorus in Water and Their Removal Efficiency [D]. Beijing forestry university.

Wang, N., Wang, C., 2018. Effects of microcystin-LR on the tissue growth and physiological responses of the aquatic plant Iris pseudacorus. L. *Aquat. Toxicol.* 200, 197–205.

Wang, Z., Zhang, J., Li, E., Zhang, L., Wang, X., Song, L., 2017. Combined toxic effects and mechanisms of microsystin-LR and copper on *Vallisneria Natans (Lour.) Hara* seedlings. J. Hazard Mater. 328, 108–116.

Wang, Peifang, You, Guoxiang, Hou, Jun, Wang, Chao, Xu, Yi, Miao, Lingzhan, Tao, Feng, Zhang, Fei, 2018. Responses of wastewater biofilms to chronic CeO_2 nanoparticles exposure: structural, physicochemical and microbial properties and potential mechanism. Water Res. 133, 208–217.

Weiwei Wang, B.Q., Zhao, Panheng, 2017. The activity of acid phosphatase in oats with different phosphorus efficiency was different under low phosphorus stress. J. North. China 5, 55–58.

Wen, M., Li, K., Wang, C., 2008. Effects of nutrient level on growth of *Vallisneria atans* in water. Res. Environ. Sci. 21 (1).

Wiegand, C., Pflugmacher, S., 2005. Ecotoxicological effects of selected cyanobacterial secondary metabolites a short review. Toxicol. Appl. Pharmacol. 203 (3), 201–218.

Xu, R., Hilt, S., Pei, Y., Yin, L., Wang, X., Chang, X., 2015. Growth phase-dependent allelopathic effects of cyanobacterial exudates on *Potamogeton crispus L.* seedlings. Hydrobiologia 767 (1), 137–149.

Yin, L., Huang, J., Li, D., Liu, Y., 2005. Microcystin-RR uptake and its effects on the growth of submerged macrophyte *Vallisneria natans (lour.) Hara*. Environ. Toxicol. 20 (3), 308–313.

Zhang, Y., 2014. Molecular Regulation of Plant Acid Phosphatase Induced by Low Phosphorus Stress. Tsinghua University.

Zhao, Y., Fang, Y., Jin, Y., Huang, J., Ma, X., He, K., He, Z., Wang, F., Zhao, H., 2015. Microbial community and removal of nitrogen via the addition of a carrier in a pilot-scale duckweed-based wastewater treatment system. Bioresour. Technol.

179, 549–558.
Zhao, Z., Zhirui, Q., liling, X., Dan, Z., Javid, H., 2018. Dissipation characteristics of pyrene and ecological contribution of submerged macrophytes and their biofilms-leaves in constructed wetland. Bioresour. Technol. 267, 158–166.
Zheng, G., Xu, R., Chang, X., Hilt, S., Wu, C., 2013. Cyanobacteria can allelopathically inhibit submerged macrophytes: effects of Microcystis aeruginosa extracts and exudates on Potamogeton malaianus. Aquat. Bot. 109, 1–7.
Zhu, Guangwei, Wang, Fang, Gao, Guang, Zhang, Yunlin, 2008. Variability of phosphorus concentration in large, shallow and eutrophic lake Taihu, China. Water Environ. Res. 80, 832–839.